The Astrophysical Journal, 752:70 (10pp), 2012 June 10 doi:10.1088/0004-637X/752/1/70

OBSERVATIONS OF MULTIPLE SURGES ASSOCIATED WITH MAGNETIC ACTIVITIES IN AR 10484 ON 2003 OCTOBER 25

Wahab Uddin[1], B. Schmieder[2], R. Chandra[3], Abhishek K. Srivastava[1], Pankaj Kumar[4], and S. Bisht[3]
[1] Aryabhatta Research Institute of Observational Sciences (ARIES), Nainital, India; wahab@aries.res.in
[2] LESIA, Observatoire de Paris-Meudon, 92195, Meudon Cedex, France
[3] Department of Physics, DSB Campus, Kumaun University, Nainital 263002, India
[4] Korea Astronomy and Space Science Institute (KASI), Daejeon 305-348, Republic of Korea
Received 2011 December 30; accepted 2012 April 9; published 2012 May 25

ABSTRACT

We present a multi-wavelength study of recurrent surges observed in Hα, UV (*Solar and Heliospheric Observatory* (*SOHO*)/EIT), and Radio (Learmonth, Australia) from the super-active region NOAA 10484 on 2003 October 25. Several bright structures visible in Hα and UV corresponding to subflares are also observed at the base of each surge. Type III bursts are triggered and *RHESSI* X-ray sources are evident with surge activity. The major surge consists of bunches of ejective paths forming a fan-shaped region with an angular size of ($\approx$65°) during its maximum phase. The ejection speed reaches up to $\sim$200 km s^{-1}. The *SOHO*/Michelson Doppler Imager magnetograms reveal that a large dipole emerges from the east side of the active region on 2003 October 18–20, a few days before the surges. On 2003 October 25, the major sunspots were surrounded by "moat regions" with moving magnetic features (MMFs). Parasitic fragmented positive polarities were pushed by the ambient dispersion motion of the MMFs and annihilated with negative polarities at the borders of the moat region of the following spot to produce flares and surges. A topology analysis of the global Sun using Potential Field Source Surface shows that the fan structures visible in the EIT 171 Å images follow magnetic field lines connecting the present active region to a preceding active region in the southeast. Radio observations of Type III bursts indicate that they are coincident with the surges, suggesting that magnetic reconnection is the driver mechanism. The magnetic energy released by the reconnection is transformed into plasma heating and provides the kinetic energy for the ejections. A lack of a radio signature in the high corona suggests that the surges are confined to follow the closed field lines in the fans. We conclude that these cool surges may have some local heating effects in the closed loops, but probably play a minor role in global coronal heating and the surge material does not escape to the solar wind.

Key words: magnetic reconnection – Sun: chromosphere – Sun: corona – Sun: flares – Sun: magnetic topology – sunspots

Online-only material: color figures

1. INTRODUCTION

Solar surge is a collimated ejection of plasma material from the lower solar atmosphere into the corona. These ejecta also exhibit episodic heating and cooling, therefore, they may be visible in the range of emissions from Hα to EUV/UV and X-rays, and can be abbreviated in general as solar jets (Schmieder et al. 1995). The surges may have an initiation velocity of $\sim$50 km s^{-1}, which may further increase up to a maximum value of 100–300 km s^{-1}, and these surges may reach up to heights of 10–200 Mm or even more (Sterling 2000). The lifetime of surges is about 30 minutes, and they can be recurrent with a period of an hour or more (Schmieder et al. 1984, 1995). Usually, the surge is confined to one or several narrow threads of magnetic fields embedded in the plasma that shoot out above the solar surface. However, such surges are mostly associated with the flaring regions and the sites of solar transients where recurrent magnetic reconnection is dominant. The evolution of solar surges has been studied comprehensively in association with magnetic field emergence and cancellation, as well as flaring activities of the solar atmosphere where such plasma jets also appeared twisted and spiraled (e.g., Schmieder et al. 1994; Chae et al. 1999; Yoshimura et al. 2003; Liu & Kurokawa 2004 and references therein).

The solar surges may occur in regions of emerging magnetic fluxes in the vicinity of satellite spots (Rust 1968; Roy 1973; Kurokawa & Kawai 1993). Often these surges are associated with flares (Schmieder et al. 1988, 1995; Uddin et al. 2004; Chandra et al. 2006), and magnetic reconnection may be responsible for the acceleration as well as the heating of the plasma. Another kind of reconnection could occur due to the collision of opposite polarity magnetic fluxes in the "moat region" (Brooks et al. 2007). Small, moving magnetic features (MMFs; Harvey & Harvey 1973; Sainz Dalda & López Ariste 2007; Kitiashvili et al. 2010) are observed as moat regions. The formation of MMFs is closely related to the fragmentation and disintegration of sunspot magnetic fluxes. Recent studies show that the amount of magnetic flux lost by the sunspots is similar to the flux transported in the moat region (Kubo et al. 2008). The flux is annihilated at the border of the moat region, and in consequence, the subflares, jets, and surges may occur during the reconnection processes along neutral lines (Beck et al. 2007; Brooks et al. 2007, 2008; Engell et al. 2011). Theoretical models have been developed concerning canceling flux producing surges or jets. The emerging-flux model of Yokoyama & Shibata (1996) supports this kind of surge dynamics, which may be triggered due to the interaction of an emerging photospheric field with the pre-existing overlying coronal magnetic fields. Although magnetic reconnection and photospheric magnetic activities may be the key in driving many solar surges and other jets, several other mechanisms may also be responsible for the surge/jet dynamics. Pariat et al. (2010) have developed a three-dimensional reconnection model without evidence of an emerging flux. This model is able to generate untwisting

jets when a stress is constantly applied at the photosphere (Rachmeler et al. 2010). Shibata et al. (1982) and Sterling et al. (1993) have reported that the pressure pulse can trigger solar surges of moderate height in the hydrodynamic regime of the solar atmosphere. Solar surges may also be accelerated due to the whip motion of the reconnection-generated, newly formed magnetic field (Shibata et al. 1992; Canfield et al. 1996a), while the reconnection-generated explosive events may also trigger such kinds of plasma dynamics (Madjarska et al. 2009). In addition to the typical solar surges, Georgakilas et al. (1999) have observed the polar surges as cool jets at polar region without any association with transients. Recently, the cool jets and surges have also been modeled, respectively, in the polar region as well as near the boundary of a non-flaring active region due to the reconnection-generated velocity pulses in the ideal magnetohydrodynamic (MHD) regime of the solar atmosphere (Srivastava & Murawski 2011; Kayshap et al. 2012). In conclusion, the solar surges and other various types of solar jets may be excited via both, e.g., the direct magnetic reconnection processes in the emerging field regions, as well as due to the magnetohydrodynamic wave activities.

During 2003 October–November, major solar activity originated from three super-active regions, namely, NOAA AR 10484, 10486, and 10488. The active region NOAA 10484 (N05W29) evolved on 2003 October 25 and was very complex, having a $\beta\gamma\delta$ configuration. This active region has produced many recurrent surges and flare activities during its passage on the solar disk. It produced major surge activities on 2003 October 22 and 25. On October 25, we observed recurrent surges between 01:50 UT and 04:15 UT. A preliminary report on these observations has been presented in Uddin et al. (2010). In this active region, there was no evidence of strong emerging magnetic fluxes during the recurrent surges.

Many questions arise around the surge activity. What is the trigger mechanism of the surges? Are they due to reconnection with the pre-existing field lines? What are the dynamics of the magnetic boundary causing the collision of opposite polarities? Are the pre-existing field lines open or closed at the periphery of the active region? Commonly, outflows are observed at the periphery of active regions (Harra et al. 2008; Del Zanna 2008). McIntosh & De Pontieu (2009) claimed that dynamic chromospheric spicules in the outskirts of active regions are related to these outflows. Warren et al. (2011) and Ugarte-Urra & Warren (2011) claimed that there is no direct relationship between these two populations of structures, i.e., the hot and cool loops maintained, respectively, at mega/sub-mega-Kelvin temperatures. The question arises whether or not these observed surges in AR 10484 may participate in the commonly observed outflows in the outskirts of active regions. To understand this issue, statistical studies should be done to find if any relationship between these cool jets and the outflows of hot plasma commonly observed at the periphery of active regions exists. However, this topic is out of the scope of the present work.

In this paper, we present a detailed multi-wavelength study of recurrent surges and their associated events (e.g., flares) as occurred in AR 10484. In Section 2, we present the details of the data sets used in this study. The multi-wavelength evolution of the surges and their association with subflares are described in Section 3. In Section 4, we describe the magnetic field evolution of an active region before and during the surges and associated flares. We discuss the possibility for a decaying active region and its magnetic activities to produce surges, and in the last section, we present our conclusions from our results in the frame of the above questions and on the possible trigger of the surges: wave or reconnection.

2. OBSERVATIONAL DATA SETS

The data sets used for our present study have been taken from the following sources.

Hα Data. The Hα observations of the flare and associated surges were carried out at ARIES, Nainital, India by using the 15 cm f/15 Coudé solar tower telescope equipped with Hα filter. The image size was enlarged by a factor of two using a Barlow lens. The images were recorded by a 16 bit 576 × 384 pixel CCD camera system having a pixel size of 22 μ^2. The resolution of the images is $1''$ pixel^{-1}. The cadence for the images is ∼15–20 s.

Solar and Heliospheric Observatory (SOHO)/Michelson Doppler Imager (MDI) Data. To understand the evolution of the magnetic complexity of the active region, we use *SOHO*/MDI data. The magnetic field data were taken from the *SOHO*/MDI instrument (Scherrer et al. 1995). The cadence of images is 96 minutes and the pixel resolution is $1''.98$.

SOHO/EIT Data. SOHO/EIT (Delaboudinière et al. 1995) observes the full-disk Sun with a cadence of 12 minutes and a pixel resolution of $2''.5$. It observes in four spectral bands centered on Fe IX/X (171 Å), Fe XII (195 Å), Fe XV (284 Å), and He II (304 Å). For our current study, we used the 171 Å data.

X-Ray Data. To understand the evolution of flares and associated surges, we reconstructed X-ray images from the *Reuven Ramaty High-Energy Solar Spectroscopic Imager* (*RHESSI*; Lin et al. 2002). We reconstructed the images in the 6–12 keV energy band from collimators (3F to 9F) using the *CLEAN* algorithm, which has a spatial resolution of ≈$7''$ (Hurford et al. 2002).

3. MULTI-WAVELENGTH OBSERVATIONS OF RECURRENT SURGES AND ASSOCIATED FLARES

The multi-wavelength evolution of the observed solar surges and their association with flares are described in the following subsections.

3.1. Temporal Variations of Hα Surges and Flares

The ARIES Hα images during the surge activities on 2003 October 25 from NOAA AR 10484 are presented in Figure 1. They show the dynamic evolution of the recurrent surge activity from 01:50 UT to 04:15 UT. During the above-mentioned time period, we observed several surges in Hα. The surge activity occurred in the following satellite sunspots of the active region NOAA AR 10484.

Seven surges (Surge 1 to Surge 7) were identified (Figure 1, see the arrows). Four of them were clearly associated with Hα brightenings. To investigate in more detail the surge evolution and the Hα brightenings at their footpoints, we computed the Hα relative intensity profile of the brightenings, the time of the Hα brightening maxima, the onsets of surges, and the time when the surge vanishes (Figure 2 and Table 1).

In Figure 2, we also present the *GOES* soft X-ray light curve obtained by the full-disk integration (top panel) and the *RHESSI* satellite thermal emission (6–12 keV) of the AR 10484 (middle panel). Unfortunately the latter curve has large time gaps, however, we are able to identify two flares at ∼3:00 UT and at ∼4:00 UT. By comparing the three light curves of Figure 2, we conclude that all the C class X-ray flares of the *GOES* curve (Flares 1, 2, and 3 with three bumps) occur in AR 10484, except for one at 02:02 UT which is observed in the

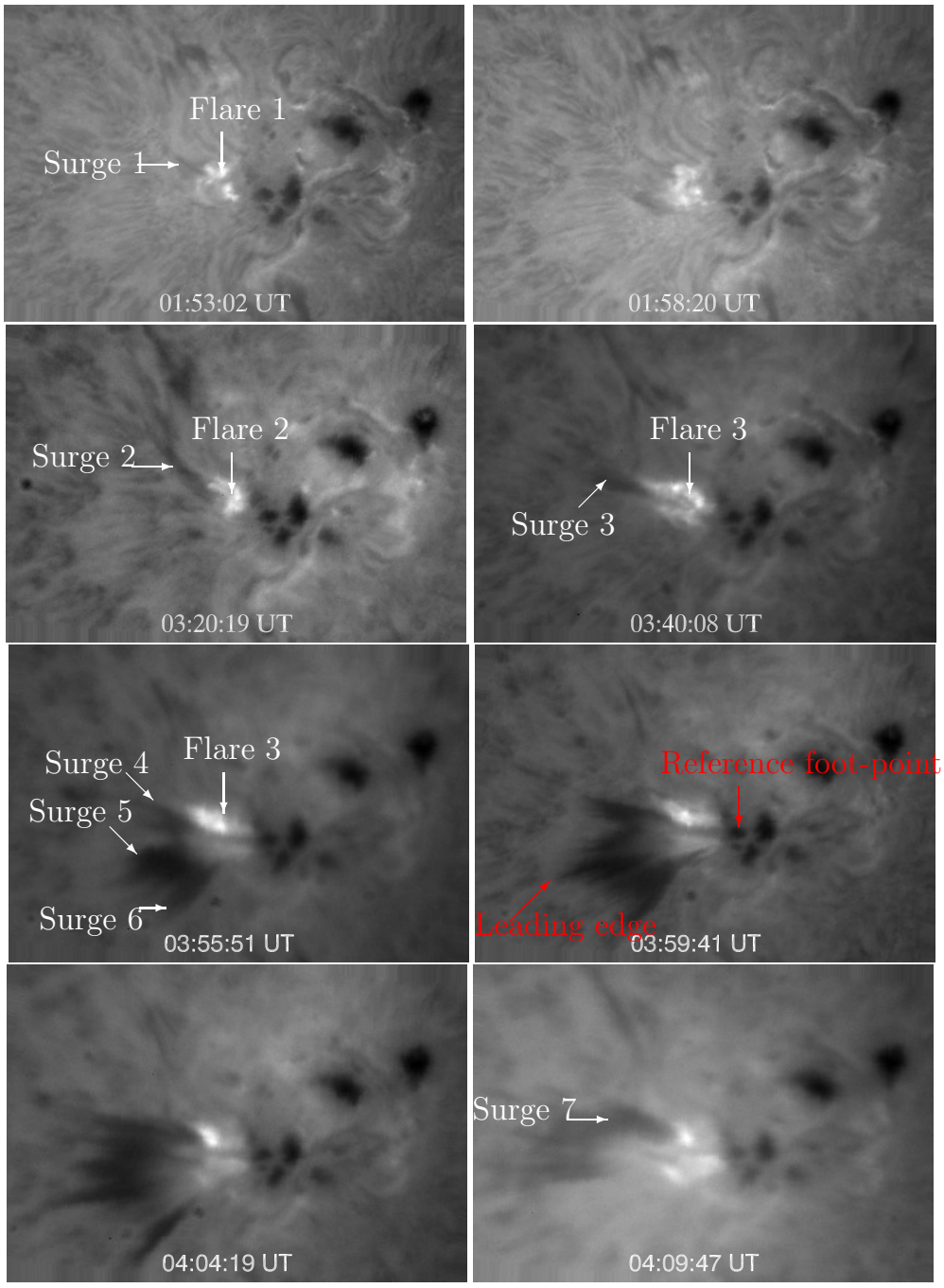

Figure 1. Hα image sequence showing the recurrent flare/surge activities on 2003 October 25 in AR 10484. The field of view of each image is 320″ × 200″.
(A color version of this figure is available in the online journal.)

Table 1
Details of the Surges and Flares

Name of Surge	Surge Onset	Hα Max Intensity	Max *GOES*	Flare Class	No. of Flare	Max *RHESSI*	Max Surge Length	Type III
1	1:50	1:50	1:57	C1.2	1	No	2:10	1:55–58
2	3:05	<3:09	3:00	C2.6	2	3:00	3:30	3:00
3	3:36	3:30–39	3:35–3:39	C3.9	3 (bump 1)	No	3:40	3:35–3:45
4	3:50	3:52	3:52	C3.4	3 (bump 2)	No	4:00	...
5	3:42	3:40	3:40	C3.9	3 (bump 1)	No	4:05	3:35–3:45
6	<3:55	...	...	...	...	No	4:09	...
7	4:09	4:10	3:57	C3.6	3 (bump 3)	<4:00	4:20	4:20

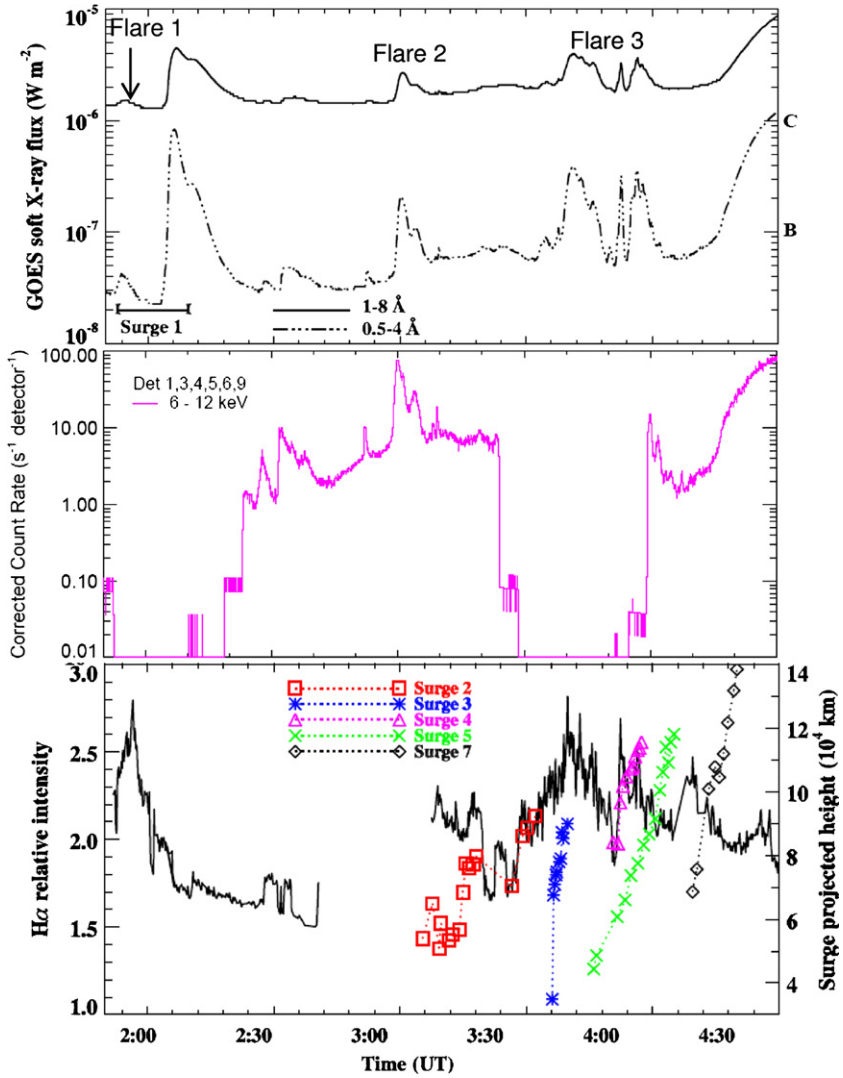

Figure 2. *GOES* soft X-ray flux (top panel) profiles in two different wavelengths on 2003 October 25. The Hα relative intensity profile is well correlated with the *GOES* flux (bottom panel). There was a Hα data gap in between 02:40 and 03:05 UT. There were recurrent small surge activities associated with flares at ∼01:55 and between 03:00 UT and 04:30 UT (Flares 1, 2, and 3). The C4.3 flare during 02:02–02:12 occurred in another AR NOAA 10486 located at the eastern limb. The length–time plot of the surges is shown and demonstrates the surge–flare relationship.

(A color version of this figure is available in the online journal.)

neighboring AR 10486. We present in Table 1 the class of the flares. We reconstructed images of *RHESSI* in the low-energy band (6–12 keV) where there are enough counts.

To understand the location of the X-ray sources with Hα brightenings, we coaligned the Hα data with the *RHESSI* thermal source. The contours of the X-ray sources are drawn in two Hα images shown in Figure 3. The location of the X-ray sources coincides with the Hα brightened footpoint for the two surges corresponding to the two flares observed by *RHESSI* (Flare 2 and Flare 3 with three bumps). It demonstrates the cospatiality of the thermal sources and the Hα brightenings.

3.2. Spatial Variations of Hα Surges

We describe in detail each surge shown in Figure 1 and give quantitative results in Table 1. We have calculated for each surge its extension versus time from the brightened footpoint to its leading edge and its speed. These results are shown in Figure 2 (bottom panel) and in Table 1.

Surge 1 was a small ejection of plasma in the northeast direction, and was associated with Flare 1 and an Hα brightening (Figure 1). Due to the unavailability of the high-resolution Hα observations, we could not see its evolution in detail. Surge 2 started around 03:06 UT in the northeast direction, increased within two periods, and finally decayed around 03:30 UT. This surge was associated with Flare 2(C2.9), as well as with an Hα brightening at its footpoint. Surge 3 started very impulsively around 03:36 UT, with a rapid enhancement of an Hα brightening (see Figure 2). The plasma was ejected in the northeast direction, however, slightly east in comparison to the direction of the previous surges. This surge decayed in four minutes around 03:40 UT. The speed of this surge expansion is estimated to be 200 km s^{-1}, which is the faster. When the Hα brightening reached its maximum, the surge was decaying. It could be associated with the first bump of Flare 3 (Flare 3, bump 1). Similarly, Surge 4 started to erupt around 03:45 UT in the northeast direction from the triggering site of the recurrent surges during the impulsive and maximum phase of the Hα brightening.

At 03:55 UT, cotemporally to Surge 4, Surges 5 and 6 have already started to erupt in the east and southeast directions. Surge 5 is bigger than Surge 6, and more elongated in size. After some

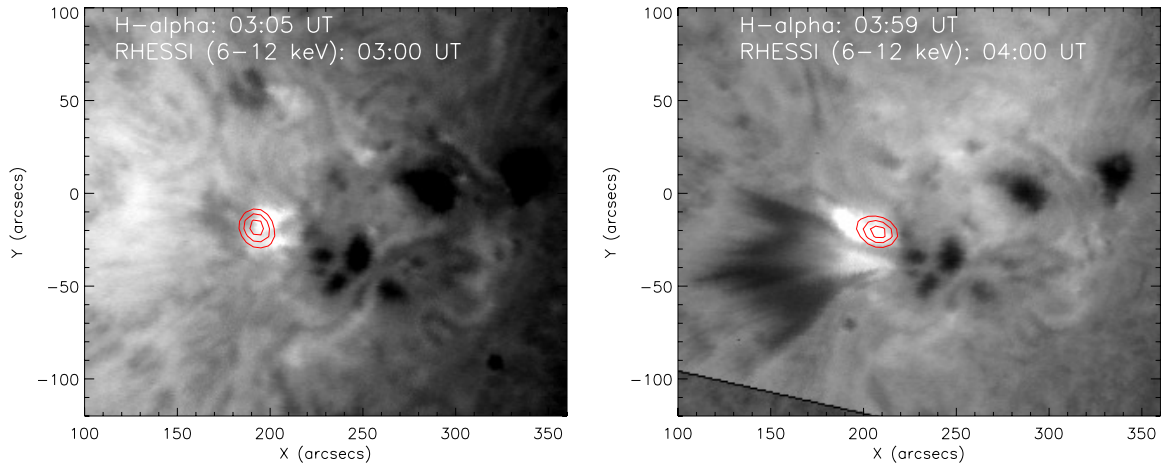

Figure 3. Hα images overlaid by *RHESSI* 6–12 keV contours during Flare 2 and Flare 3 (bump 3) The contour levels are 50%, 70%, and 90% of the peak intensity.
(A color version of this figure is available in the online journal.)

time, they appeared as a single surge forming together a fan-type dark structure. Surges 5 and 6 were not associated with intense brightenings at their footpoints. However, during the surge onset period, we found faint brightenings. Possibly the flare brightening may be hidden by the dark surge material, or it may be associated with the first bump of Flare 3.1. Thereafter, they merge with each other, and individual surges were no longer resolved. We could only calculate the length of Surge 5 as the contrast of Surge 6 was comparatively low. The length–time plot of Surge 5 shows that the surge erupts after Flare 3. Surge 7 started around 04:09 UT, again in the east direction, and was initiated from an Hα brightening corresponding to Flare 3.3. Surge 7 reached the largest height compared to the other surges. The maximum projected length in the case of Surge 7 is around 140 Mm and its speed is close to 100 km s^{-1}.

We conclude that the surge onsets were commonly associated with the impulsive phase of the *GOES* flares and reached their maximum length during the decay of Hα brightenings. Their velocities are between 25 and 200 km s^{-1}.

3.3. SOHO/EIT Observations and Topology Analysis

To compare the Hα brightenings and the coronal brightenings visible in EIT, as well as surges, we overlaid EIT contours over the Hα images at four instances. The results are shown in Figure 4. At 03:24 UT, 03:48 UT, and 04:12 UT, the EIT bright regions are elongated structures and closely cospatial with the Hα surge footpoint brightenings even though they did not correspond to the onsets of the flares. The heating indicated by the brightenings in multi-wavelengths is local and nearly cospatial. The bright Hα brightenings are possibly parts of the surges, as suggested previously (Schmieder et al. 1984) by looking at the Doppler shifts of such structures, which show a continuity in the Doppler-shift pattern between bright and dark structures. We would need to have information on the Doppler shifts all along the structures to confirm that bright and dark bundles belong to a unique structure.

An interesting feature is the shape of the loops visible in EIT before the surge activity. Figure 5 displays the *SOHO*/EIT 171 Å image at 01:00:14 UT. The dotted "V"-shaped line in the east direction indicates a fan-shaped structure of magnetic field lines, which is similar to the fan shape of the bunches of Surges 4, 5, and 6. All the Hα surges erupted in the same cone direction.

A question arises: are the field lines inside the fan open or closed? We used the Potential Field Source Surface extrapolation code to derive the global structure of the Sun on 2003 October 25. Figure 6 shows that the bunches of field lines in the fan are in fact closed field lines linking the two active regions: AR 10484 and AR 10486.

In Figure 4, the Hα image at 03:59 UT is overlaid by MDI contours. This figure shows that the footpoints of the surges are in a mixed polarity region dominated by a positive polarity. It is at the edge of the spot of the negative main polarity of the region. The region of the ejection of the surges is located between magnetic field lines on the east side of the active region and the active region itself overlaid by close loops. It means that there may be separatrix or quasi-separatrix layers (QSLs) in that region. Field lines easily change connectivity according to the photospheric motions of the mixed polarities. It is a favorable region for reconnection. We suggest that the reconnection is done successively in different locations along the separatrix from a northern point to a southern one. The material of the surge would escape along the pre-existing field lines, which make a fan-shaped structure similar to the EIT loops. The reconnection would locally heat the plasma in these reconnected field lines up to 1 MK. These events are transients and may participate in the global coronal heating only with a minor effect.

3.4. Radio Observations

Figure 7 (bottom panel) shows the dynamic radio spectrum of Learmonth observatory in the frequency range 25–180 MHz. During the maximum phase of recurrent surge activities, a series of Type III bursts has been observed (Table 1). We noticed two Type III bursts during the maximum of Surge 1 before 02:00 UT. During Surge 2, two sets of Type III bursts are evident, respectively, around 03:30 UT and 03:40 UT. Type III radio bursts generally represent the escaping electrons along open field lines (Dulk et al. 1979; Nitta & De Rosa 2008). The appearance of recurrent Type III bursts during the peak evolutionary phases of the surges may most likely be the signature of the generation of non-thermal particles due to reconnection episodes. It may be most plausible during the initiation of recurrent surge activity and the eruption of surge material that the magnetic field lines come closer and reconnect. Due to the reconnection, the energetic particles are produced and

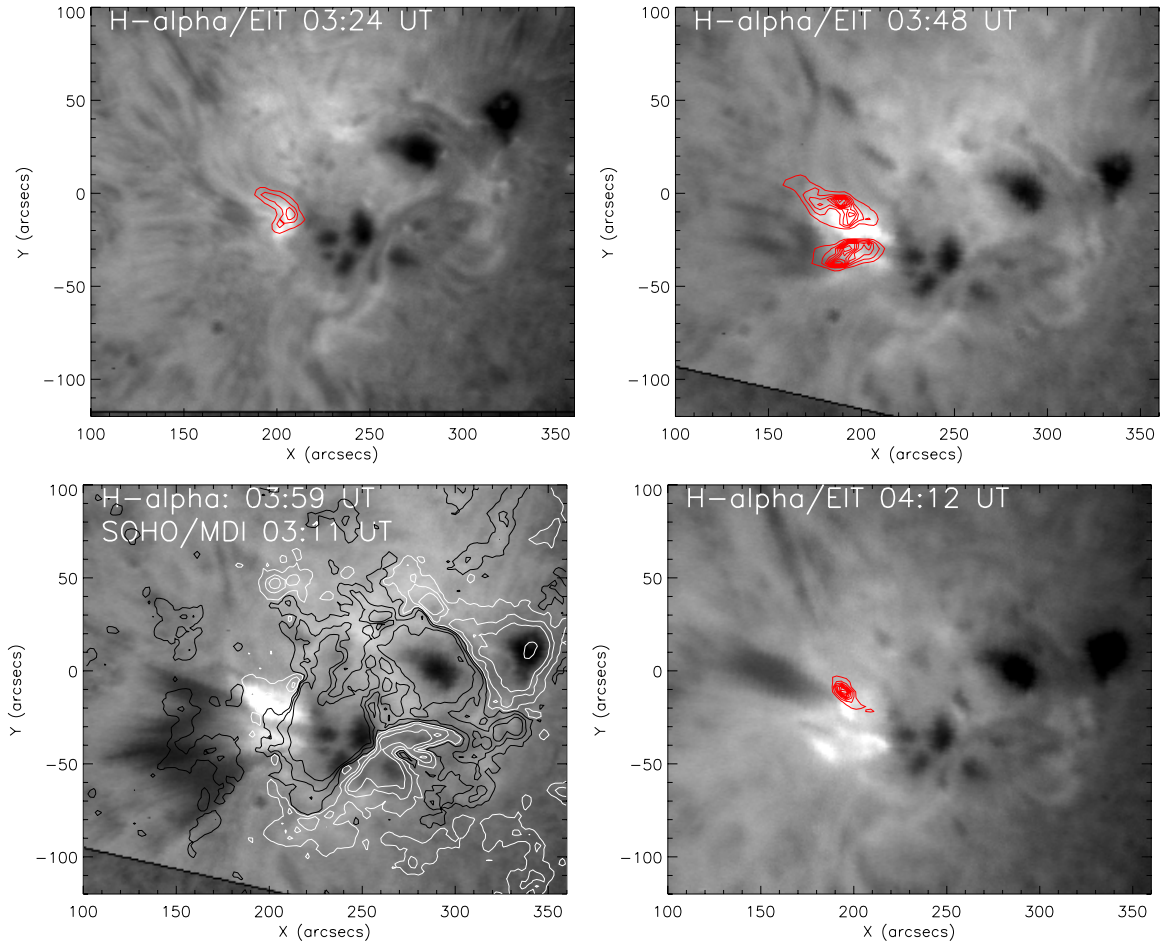

Figure 4. Hα images showing the flares and surge eruptions overlaid by the *SOHO*/EIT 171 Å contours for three different times (top and bottom right panel). The bottom left image shows an Hα image overlaid by MDI contours (white contours show the positive polarity whereas black contours indicate the negative polarity).
(A color version of this figure is available in the online journal.)

hence we observe the series of Type III radio bursts. Therefore, the presence of recurrent Type III bursts provides evidence of multiple magnetic reconnections at the activity site and bulk plasma acceleration along the field lines forming the surges. No Type III bursts have been identified in WIND satellite data, as has been shown by other authors for similar events (Bentley et al. 2000). Therefore, it confirms that the accelerated particles are reaching only to the low corona, as suggested by the radio frequency range (∼0.2, 0.3 solar radii). These particles are certainly following the system of large loops existing between the two active regions already mentioned in the previous section. These transient cool jets and associated particles are confined in close loops and cannot play an important role in the outflows observed commonly at the periphery of active regions in open field and definitively not participate in the solar wind.

4. MAGNETIC FIELD ACTIVITY RELATED WITH RECURRENT SURGES

In order to understand the relation between the recurrent surge activity and the magnetic field configuration of the region, we present the evolution of the magnetic field before, during, and after the surges (Figure 8). From MDI time series data, we see that a large bipole emerged ahead of a remnant active region as it crossed the limb. On October 18–20, the two main polarities of the emerging bipoles have a "tongue shape" as it is frequently observed during strong emergence (Chandra et al. 2009). The polarities of the old active region broke into many segments in the surrounding of the bipole and created the δ configuration of the AR 10484. This is evident as a largely extended negative polarity area surrounded by positive polarities in the active region. On October 22, the polarities already started to disperse and the active region entered in a decay phase. Figure 8 (top) shows the MDI magnetogram on 2003 October 24 at 14:23 UT before the surge activity. Opposite polarities surrounding the main polarities escape radially away from the spots. Around the left/right (negative/positive) main polarity, there is a ring of opposite polarities (positive/negative), respectively. Such a ring is observed successively on October 22 and on October 24 at 14:23 UT. This is the scenario of the building up of magnetic activity and complexity in and around the origin site of recurrent solar surges in AR 10484.

During the decay phase of sunspots there is a radial dispersion of the flux, with radial "sea serpent" structures with positive and negative polarities forming a ring of polarities that progressively reaches the network. This region surrounding the spot is called a moat region (Harvey & Harvey 1973). The polarities that are present in this moat region are in the dynamics of the dispersion. Looking at the MDI time series data, we see that this ring of polarities appears several times during the dispersion phase of the magnetic fluxes. During this time, some small fluxes were escaping from the negative/positive main polarity and most likely canceled with the moat polarities. This phenomena is a

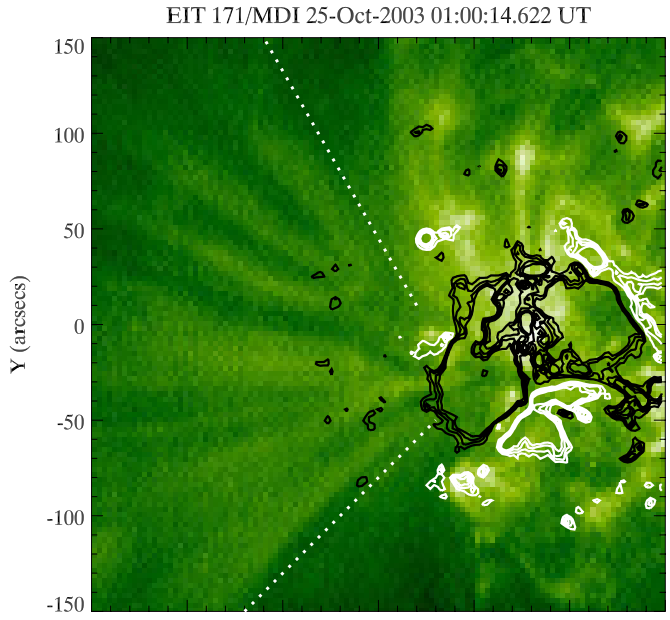

Figure 5. *SOHO*/EIT 171 Å image overlaid by the MDI contours (white shows the positive polarity whereas black indicates the negative polarity). The dotted lines indicate the fan-shaped structure of field lines over the activity site before the flare and surge activities.

(A color version of this figure is available in the online journal.)

common process to decrease the flux during the decaying phase of an active region. The enlarged part of the active region, where the surges originated, is displayed in Figure 8 (bottom).

We notice that the positive polarity P0 is submitted to the ambient dispersion process. P0 broke into three pieces, i.e., P2, P3, and P4 on October 25 at 01:35 UT. From the main negative polarity, a small negative polarity N1 escaped and disappeared on October 25 at 06:23 UT. This negative polarity (N1) was cancelled with parts of small P2 and P3 polarities. The cancellation of P0 was done in successive annihilations of positive and negative fluxes during the spatial expansion of main polarities. This annihilation occurs very close to the inversion line in close proximity to P2, P3, P4, N1, and the main negative polarity. We also followed the evolution of the P1 and N0 polarities with time and found that these polarities are increasing in size as well in magnitude, and are coming closer to each other for cancellation.

We computed the variation of magnetic fluxes in the region of these surges. For this purpose, we selected a box as shown in Figure 8. The temporal variation of positive, negative, and total fluxes before, during, and after the surge activity inside the box is shown in Figure 9. The plot shows that the positive flux increases before the surge activity due to the emergence of positive ring polarities. On the other hand, during the surge activity (shown by the vertical lines in Figure 9), we found the decrement in the positive, negative, and total flux. The constant decreasing negative flux demonstrates that the active region is in a decay phase. The decrease of the total flux at the bottom of surges indicates that the flux cancellation is an ongoing process, which would be an important factor for the triggering of solar surges. However, it is difficult to detect the decrease of the negative flux associated with the cancellation field at the base of the surge because the decrease of such a flux is one order of magnitude less according to the decrement of positive flux.

Under the baseline of our interpretation based on morphological investigation of MDI data as well as temporal variation

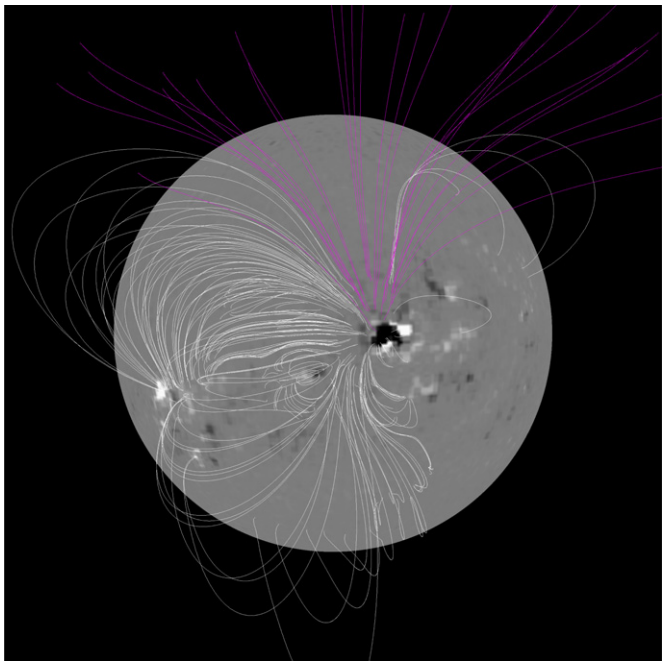

Figure 6. Potential Field Source Surface extrapolation overplotted at the *SOHO*/MDI full-disk map on 2003 October 25 on 00:04 UT, which shows the large-scale field connectivity of two active regions as well as the topology of magnetic field near the surge productivity site in AR 10484.

(A color version of this figure is available in the online journal.)

of the magnetic fluxes, it may also be quite possible that the flux cancellation could be a signature of submergence of the magnetic polarities. Therefore, the energy released by reconnection in the low solar atmosphere would be transformed into thermal heating and kinetic energy. These underlying processes of surges are starting again when the ring of opposite polarities emerges around the main spots. Another important reason that such cancellation leads to surge activity is the existence of the QSLs, a region where field lines can change connectivity.

In the present study under the baseline of our observations, we found the emergence and fragmentation of magnetic polarities, and thereafter their cancellation with the main magnetic polarities that trigger the recurrent surges and associated energy release (heating) at their footpoints. Figure 10 displays the schematic cartoon showing the surge association due to the reconnection of the neighboring field lines (i.e., positive) with the opposite polarity field region. The "X" symbol shows the reconnection point in between opposite polarity field regions.

5. DISCUSSION AND CONCLUSIONS

In the present paper, we outline a multi-wavelength study of seven recurrent surges and associated flare brightenings on 2003 October 25 from the active region NOAA AR 10484. For this study, we use ARIES Hα, *SOHO*/EIT, MDI, and *RHESSI* observations. Out of seven surges, five surges were associated with footpoint brightenings and corresponding flare energy release. In the case of Surges 5 and 6, we could not notice the footpoint brightening. One possibility for not seeing footpoint brightening is that these surges are very dynamic and extended. Also, due to the large area of these surges, the compact footpoint brightening may be hidden in the cool plasma eruption. The length–time plots of brightening-associated surges indicate that the length is increasing or sometimes decreasing (as in the case of Surge 2) with the increment or decrement of the

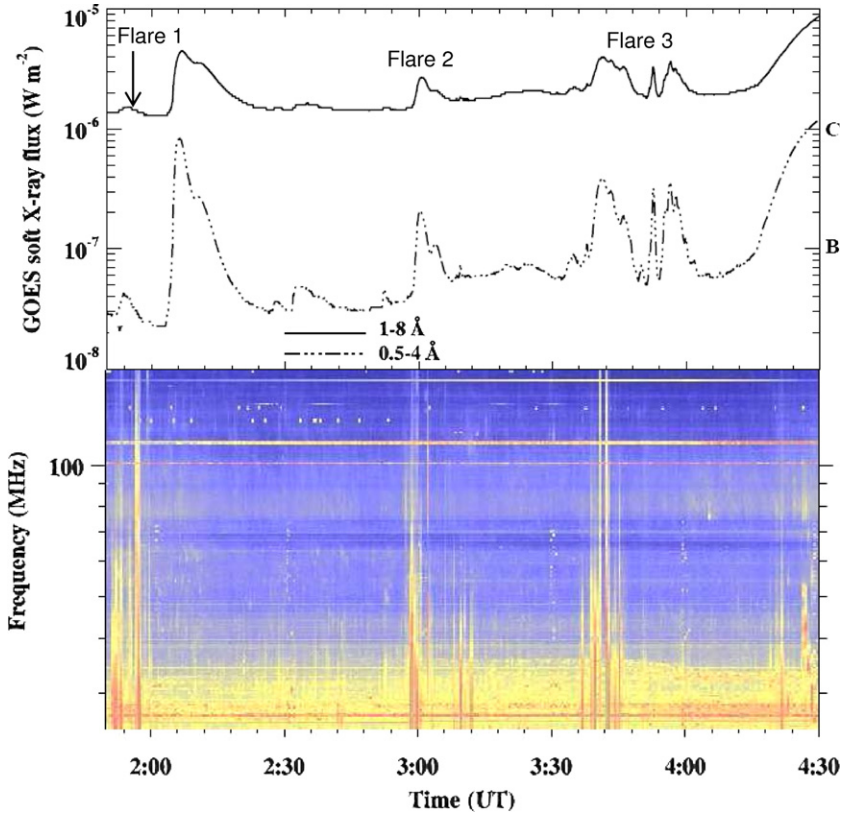

Figure 7. *GOES* soft X-ray light curve and Radio Type III bursts (Learmonth).
(A color version of this figure is available in the online journal.)

brightness at the footpoint. This is the evidence that compact energy release at the base is pumping the plasma material in the form of a surge. All the surges are ejected in the northeast to southeast direction. The speed of the surges is between 25 and 200 km s^{-1}. This kind of large velocity has been observed in spicules Type II in Ca H as reported by De Pontieu & McIntosh (2010). They claimed that they can follow the up flows in hot structures (1–2 MK) which could participate in the coronal heating. We cannot confirm their findings even if hot material (1 MK) is observed. Recently, the hot plasma up flows were also detected near the boundary of active regions, which may be potential candidates for coronal heating (De Pontieu et al. 2011). Such types of jets, surges, and confined plasma dynamics have been modeled recently in the form of the evolution of slow shocks that could carry the hot plasma material followed by the cool plasma in the underpressure region in magnetic flux tubes (Srivastava & Murawski 2011, 2012; Kayshap et al. 2012). After all, in the present observations, the hot plasma is detected at the base of the cool jets and not at the top. The shock mechanism cannot be at work in the present situation. Both hot and cool plasma follow field lines belonging to the same system joining two active regions. This plasma is not in open field lines, and therefore, will not implement the commonly observed outflows in the outskirts of the active regions which could participate in the initiation of the solar wind (Harra et al. 2008; Del Zanna 2008).

The MDI magnetograms reveal the positive flux of opposite polarities around the main spots. This behavior could indicate that the active region is in a decay phase with the presence of a moat region. The polarities are very much fragmented in this moat region. The dispersion motion pushed the parasitic positive polarities to merge with negative polarities in the moat region. The positive parasitic polarity changes shape, breaking into pieces, and cancels with neighboring opposite polarities during the dispersion of the dipoles of the moat. The cancellation of flux initiates the surges. The horizontal motion of the polarities in the moat region is important for pushing the opposite polarities together and forces the reconnection. The field lines of the sunspot penumbra reconnect with the pre-existing open field external to the active region. It is frequently observed that surges occur at the periphery of active region close to parasitic polarities (Kurokawa et al. 2007; Brooks et al. 2007). MHD simulations show that surges and jets occur when polarities merge close to open field lines like in coronal holes (Moreno-Insertis et al. 2008). A question subsists if the surges are produced by squeezing and compression of the plasma or by reconnection (Isobe et al. 2007). Flux cancellation at the bottom of the surges might give the power for recurrent surge activities. This scenario is supported by Yokoyama & Shibata (1996) on the basis of numerical simulations. The flares that formed near the footpoints of the surges and the Type III radio bursts that were observed during these events are evidence of magnetic reconnections (Shibata et al. 1994; Canfield et al. 1996b; Bentley et al. 2000). The presence of open field close to the active region favors the occurrence of surges and jets (Moreno-Insertis et al. 2008).

However, the formation of various types of jets (e.g., surges, coronal jets, spicules) at different spatio-temporal scales can either be driven by a direct reconnection process, or sometimes reconnection triggers them indirectly. This depends upon the height of the reconnection site as well as the local plasma and magnetic field conditions. Sterling et al. (1993) have

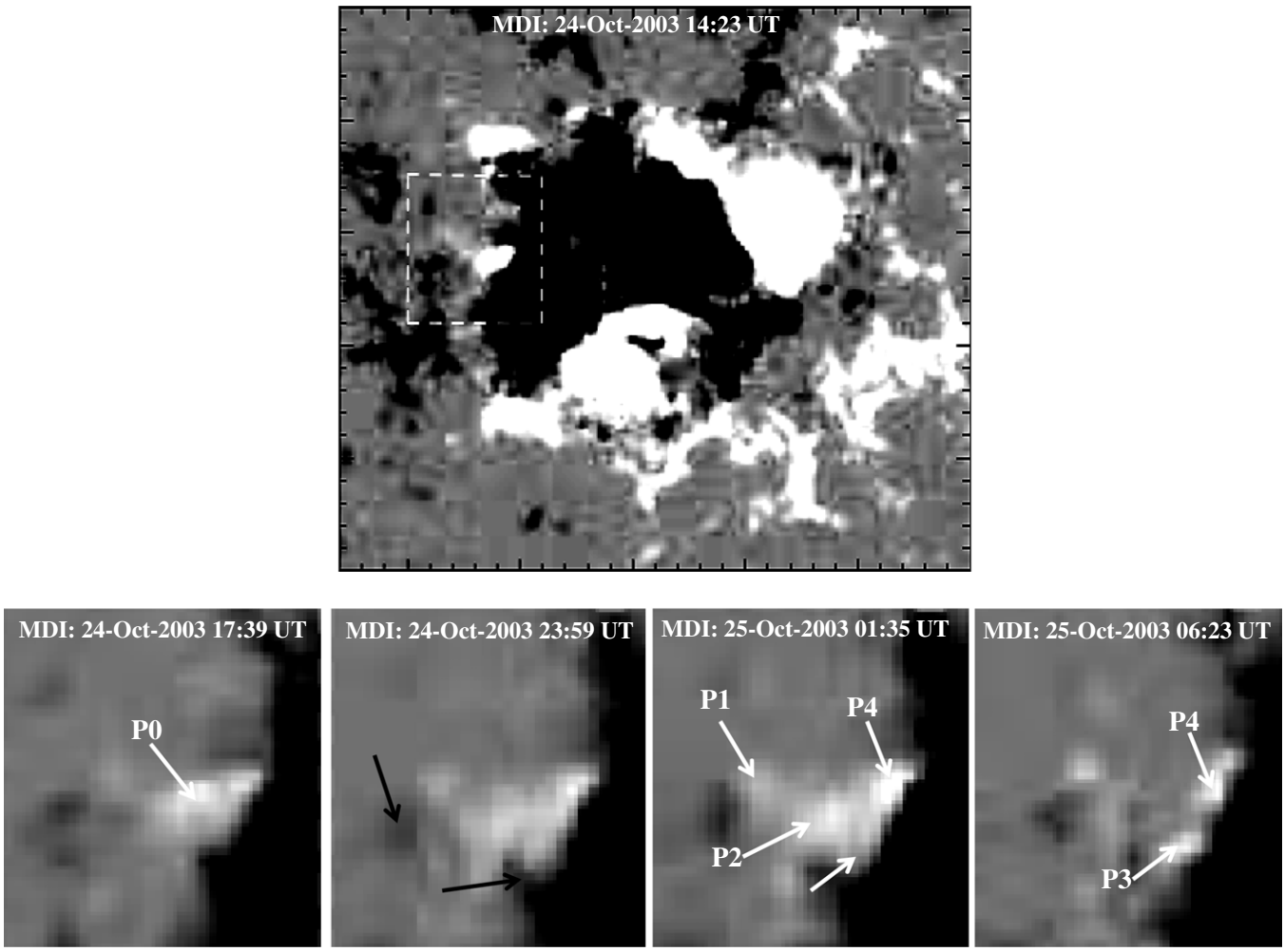

Figure 8. Magnetogram on 2003 October 24 before the surge activity showing the moat region around the main polarities (top panel) and zoom on the region of the surges (presented as a white box in the top panel) before, during, and after the surges (bottom panel). The field of view of the upper and lower images is $280'' \times 250''$ and $60'' \times 65''$, respectively.

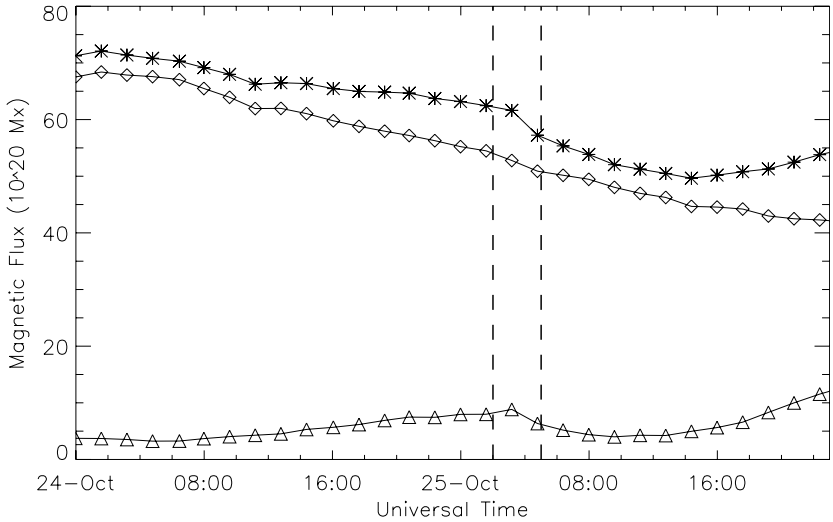

Figure 9. Temporal variation of positive (triangle), negative (diamond), and total (star) magnetic flux before, during, and after the surge activities as measured over the selected area shown in the bottom panels of Figure 8. The two vertical lines indicate the duration of surge activity.

demonstrated that the pressure pulse generated by energy release in the non-magnetized atmosphere can trigger the surge material. Recently, the cool jets and long spicules have been reported as driven by the reconnection-generated velocity pulses sufficiently evolved in the chromosphere (Srivastava & Murawski 2011; Murawski et al. 2011; Kayshap et al. 2012). However, such magnetohydrodynamic pulses and their steepening in form of localized shocks were associated mostly with non-flaring

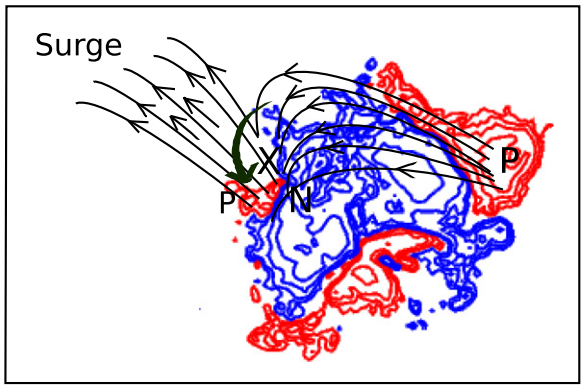

Figure 10. Schematic showing the surge initiation due to the reconnection (shown by "X") of the field lines with the opposite polarity field region, resulting in the counterclockwise motion of the negative polarity field region (indicated by thick arrow). Red contours indicate the positive polarity whereas blue ones show the negative polarity field region. Surge moves along the open field lines. (A color version of this figure is available in the online journal.)

regions, where they attain sufficient spatio-temporal scales and ambient plasma conditions for their growth and subsequently the triggering of the various types of jets. Moreover, such types of pulse-driven jets exhibit the quasi-periodic rise and fall of the plasma material. In the present observations, we get the recurrent surge jets and associated flare energy release. Photospheric magnetic field cancellation due to the fragmentation of the emerging opposite polarities and associated compact flare energy release are clearly evident, which may further release the plasma along the open field lines in the form of recurrent surges. Therefore, the recurrent flare energy release at the base of the surge locations near their footpoints generated due to photospheric reconnection may be the main cause for the surge eruptions. Collision of the magnetic polarities triggers the compact flares and associated surges. Therefore, we rule out the other causes, e.g., the generation of the pressure or velocity pulses in the surge region, evidence of some explosive event (Madjarska et al. 2009), role of the twist (Pariat et al. 2010), etc., for the presented observations of the jet formation.

In conclusion, we report on a multi-wavelength observational study of energy buildup and dynamics in the form of multiple surge eruptions associated with flares due to successive reconnections initiated by magnetic flux cancellations. However, the future multi-wavelength observations and related MHD modeling should be carried out using recent high spatial and temporal resolution observations from space (e.g., *Solar Dynamics Observatory*, *Hinode*) and complementary ground-based observations to understand the initiation, energetics, magnetic field topology, and dynamics of surges.

We acknowledge the valuable suggestions of the referee that improved our manuscript considerably. The authors thank CEFIPRA Project 3704-1 for its support of this study on "Transient events in Sun Earth System" during our bilateral collaboration. We acknowledge the space-borne instruments on board *SOHO*, *RHESSI*, and ground based Learmonth, Australia for the data used in this study. *SOHO* is an international cooperation between ESA and NASA. B.S. thanks the ISSI group (Bern) led by Klaus Galgaard on flux emergence which helped her to have a clear idea of the development of this surge activity. A.K.S. acknowledges Shobhna Srivastava for her patient encouragement.

REFERENCES

Beck, C., Bellot Rubio, L. R., Schlichenmaier, R., & Sütterlin, P. 2007, A&A, 472, 607
Bentley, R. D., Klein, K.-L., van Driel-Gesztelyi, L., et al. 2000, Sol. Phys., 193, 227
Brooks, D. H., Kurokawa, H., & Berger, T. E. 2007, ApJ, 656, 1197
Brooks, D. H., Ugarte-Urra, I., & Warren, H. P. 2008, ApJ, 689, L77
Canfield, R. C., Reardon, K. P., Leka, K. D., et al. 1996a, ApJ, 464, 1016
Canfield, R. C., Reardon, K. P., Leka, K. D., et al. 1996b, ApJ, 464, 1016
Chae, J., Qiu, J., Wang, H., & Goode, P. R. 1999, ApJ, 513, L75
Chandra, R., Jain, R., Uddin, W., et al. 2006, Sol. Phys., 239, 239
Chandra, R., Schmieder, B., Aulanier, G., & Malherbe, J. M. 2009, Sol. Phys., 258, 53
Delaboudinière, J., Artzner, G. E., Brunaud, J., et al. 1995, Sol. Phys., 162, 291
Del Zanna, G. 2008, A&A, 481, L49
De Pontieu, B., & McIntosh, S. W. 2010, ApJ, 722, 1013
De Pontieu, B., McIntosh, S. W., Carlsson, M., et al. 2011, Science, 331, 55
Dulk, G. A., Melrose, D. B., & Suzuki, S. 1979, PASA, 3, 375
Engell, A. J., Siarkowski, M., Gryciuk, M., et al. 2011, ApJ, 726, 12
Georgakilas, A. A., Koutchmy, S., & Alissandrakis, C. E. 1999, A&A, 341, 610
Harra, L. K., Sakao, T., Mandrini, C. H., et al. 2008, ApJ, 676, L147
Harvey, K., & Harvey, J. 1973, Sol. Phys., 28, 61
Hurford, G. J., Schmahl, E. J., Schwartz, R. A., et al. 2002, Sol. Phys., 210, 61
Isobe, H., Tripathi, D., & Archontis, V. 2007, ApJ, 657, L53
Kayshap, P., Srivastava, A. K., & Murawski, K. 2012, ApJ, submitted
Kitiashvili, I. N., Bellot Rubio, L. R., Kosovichev, A. G., et al. 2010, ApJ, 716, L181
Kubo, M., Lites, B. W., Shimizu, T., & Ichimoto, K. 2008, ApJ, 686, 1447
Kurokawa, H., & Kawai, G. 1993, in ASP Conf. Ser. 46, IAU Colloq. 141: The Magnetic and Velocity Fields of Solar Active Regions, ed. H. Zirin, G. Ai, & H. Wang (San Francisco, CA: ASP), 507
Kurokawa, H., Liu, Y., Sano, S., & Ishii, T. T. 2007, in ASP Conf. Ser. 369, New Solar Physics with Solar-B Mission, ed. K. Shibata, S. Nagata, & T. Sakurai (San Francisco, CA: ASP), 347
Lin, R. P., Dennis, B. R., Hurford, G. J., et al. 2002, Sol. Phys., 210, 3
Liu, Y., & Kurokawa, H. 2004, ApJ, 610, 1136
Madjarska, M. S., Doyle, J. G., & de Pontieu, B. 2009, ApJ, 701, 253
McIntosh, S. W., & De Pontieu, B. 2009, ApJ, 706, L80
Moreno-Insertis, F., Galsgaard, K., & Ugarte-Urra, I. 2008, ApJ, 673, L211
Murawski, K., Srivastava, A. K., & Zaqarashvili, T. V. 2011, A&A, 535, A58
Nitta, N. V., & De Rosa, M. L. 2008, ApJ, 673, L207
Pariat, E., Antiochos, S. K., & DeVore, C. R. 2010, ApJ, 714, 1762
Rachmeler, L. A., Pariat, E., DeForest, C. E., Antiochos, S., & Török, T. 2010, ApJ, 715, 1556
Roy, J. R. 1973, Sol. Phys., 28, 95
Rust, D. M. 1968, in IAU Symp. 35, Structure and Development of Solar Active Regions, ed. K. O. Kiepenheuer (Cambridge: Cambridge Univ. Press), 77
Sainz Dalda, A., & López Ariste, A. 2007, A&A, 469, 721
Scherrer, P. H., Bogart, R. S., Bush, R. I., et al. 1995, Sol. Phys., 162, 129
Schmieder, B., Golub, L., & Antiochos, S. K. 1994, ApJ, 425, 326
Schmieder, B., Mein, P., Martres, M. J., & Tandberg-Hanssen, E. 1984, Sol. Phys., 94, 133
Schmieder, B., Mein, P., Simnett, G. M., & Tandberg-Hanssen, E. 1988, A&A, 201, 327
Schmieder, B., Shibata, K., van Driel-Gesztelyi, L., & Freeland, S. 1995, Sol. Phys., 156, 245
Shibata, K., Ishido, Y., Acton, L. W., et al. 1992, PASJ, 44, L173
Shibata, K., Nishikawa, T., Kitai, R., & Suematsu, Y. 1982, Sol. Phys., 77, 121
Shibata, K., Nitta, N., Strong, K. T., et al. 1994, ApJ, 431, L51
Srivastava, A. K., & Murawski, K. 2011, A&A, 534, A62
Srivastava, A. K., & Murawski, K. 2012, ApJ, 744, 173
Sterling, A. C. 2000, Sol. Phys., 196, 79
Sterling, A. C., Shibata, K., & Mariska, J. T. 1993, ApJ, 407, 778
Uddin, W., Jain, R., Yoshimura, K., et al. 2004, Sol. Phys., 225, 325
Uddin, W., Kumar, P., Srivastava, A. K., & Chandra, R. 2010, in Magnetic Coupling between the Interior and Atmosphere of the Sun, ed. S. S. Hasan & R. J. Rutten (Berlin: Springer), 478
Ugarte-Urra, I., & Warren, H. P. 2011, ApJ, 730, 37
Warren, H. P., Ugarte-Urra, I., Young, P. R., & Stenborg, G. 2011, ApJ, 727, 58
Yokoyama, T., & Shibata, K. 1996, Astrophys. Lett. Commun., 34, 133
Yoshimura, K., Kurokawa, H., Shimojo, M., & Shine, R. 2003, PASJ, 55, 313